

## Development and testing of a double-row adjustable disc ridger

David A. Wandusim<sup>1\*</sup>, Emmanuel Y. H. Bobobee<sup>2</sup>, Fabrice Abunde<sup>3</sup>, Emmanuel Awuah<sup>4</sup> and Michael A. Ampomah<sup>1</sup>

Received: 9th September, 2022 / Accepted: 2nd January, 2023

Published online: 28th February, 2023

### Abstract

Ridging has been discovered as a mechanized alternative to mounding and flat-land forms in root and tuber crop production. While manual ridging is possible, evidence reveals that manual ridging is laborious and time-consuming; hence, the need to mechanise the ridging process. A double-row disc ridger was developed and tested. The approaches of functional analysis (FA) and computer-aided design (CAD) were used. The implement was fabricated from locally available materials and tools, making it an adaptable, resilient and affordable technology for small-scale farmers. The prototype was tested at three varied tractor speeds (i.e., 6 km/h, 8 km/h and 9 km/h) and disc angle from 40° – 45° to determine the draught force, fuel consumption, wheel-slip, depth and width of cut. Preliminary results indicate that optimum performance was achieved at a tractor speed of 6 km/h and disc and tilt angle of 42.5° and 25° respectively. The ridger recorded a field capacity of 1.45 ha/h and average fuel consumption of 6.3 l/ha. It was observed that increased tractor speed and disc angle resulted in increased draught force from 1.8 – 2.4 kN, increased fuel consumption from 5.2 – 7.04 l/ha and increased depth and width of cut from 30 – 40 cm and 250 – 280 cm, respectively. Wear and durability tests on different agro-ecologies are also recommended.

**Keywords:** Disc-ridger, Development, Functional-analysis, Root-crop, Performance-testing

### Introduction

It is widely acknowledged that raising the level of mechanization among smallholder farmers, who contribute 90 % of Africa's root and tuber crops, is key to increased agricultural productivity (Nanbol and Namu, 2019). While experts in African root crops (cassava) unanimously agree that mechanization is the most important intervention to increase the competitiveness of the industry (Sanginga, 2015; Diao, Silver and Takeshima, 2016; Sims and Kienzle, 2016), current research on root and tuber suggests low levels of mechanization among small-scale and commercial farming. Due to this, production practices such as tillage, planting, weed control and harvesting are done manually. This is labour intensive, time-consuming, expensive, imposes a lot of human drudgery and limits the scale of production. According to Sanginga (2015), 8-12 % of cassava roots are lost due to sub-optimal tillage methods in both small-scale and commercial farming. Because of these and other reasons, research and development of appropriate implements for smallholder farmers have been identified as a priority area in Ghana's Food and Agriculture Sector Development Policy (FASDEP) (MoFA, 2002).

In a generalised view of root crop cultivation, while it involves several unit operations, there is growing interest in tillage optimization because it consumes over 60 % of the total energy required.

Also, row-planting has become imperative with the introduction of mechanical harvesters in root crop production, which has further led to a growing research interest in tillage operations such as ridging (Amponsah *et al.*, 2014; Amponsah *et al.*, 2017). While ridging or bond-forming can be achieved manually, research by Wang *et al.* (2013) reports that manual ridging is laborious, and the quality and standard of ridging cannot be guaranteed, hence ridge building must be achieved by a ridging implement. Among the different categories/types of ridgers, disc ridgers have received considerable attention due to their ability to work in difficult soil conditions. Disc ridgers play an important role in the following farm applications: tillage operations, where it is used to produce ridges for row crop cultivation and irrigation sites where it is used to form bonds or terraces to damp and direct irrigable water or check erosion.

Recent developments show that planting cassava on ridges has the advantage of higher root yield coupled with better and easier field management and has the potential for mechanization of root and tuber production to reduce drudgery and increase the scale of production compared to planting on flatland forms and mounds (Ennin *et al.*, 2009; Amponsah *et al.*, 2017).

Studies have shown that among other ridging implements, the disc ridger is preferred mainly because of its ability to roll-over obstacles giving it impetus to work in difficult soil conditions. However, disc ridgers in the local market are prone to structural failure (frame breakages), unstable working width adjustment, and susceptible to hub-base wear, when subjected to arable soils in Ghana. Also, they produce narrow ridges suitable for horticultural crops but are inadequate for root and tuber crops. Therefore, major field operations such as planting, weed control and harvesting in root and tuber production are still carried out manually, in most developing countries.

Despite the many advantages disc ridgers have, to support small-holder farmers, there has been inadequate research and development of these ridgers locally to meet their needs. Among few researches on disc ridging implements include works done by Ennin *et al.* (2009), Nkakini and Akor (2012)

\*Corresponding author's email: wandusim@tatu.edu.gh

<sup>1</sup>Department of Agricultural Engineering, Tamale Technical University, Tamale, Ghana.

<sup>2</sup>Department of Agricultural and Biosystems Engineering, Kwame Nkrumah University of Science and Technology, Kumasi, Ghana.

<sup>3</sup>Abunde Sustainable Engineering Group (AbundeSEG), Douala Cameroon

<sup>4</sup>Nanjing Agricultural University, Nanjing, China

and Abdullah and Rahman (2019). Literature search so far shows that there has been no research report on the development and evaluation of disc ridgers in Ghana. Therefore, the advancement of research around design, development and performance evaluation of disc ridgers to enhance the mechanization of root and tuber crops in Ghana is very necessary.

The purpose of this study was to design, construct and test the performance of a two-row disc ridger using functional analysis and computer-aided design (CAD) approach. This design framework establishes the principal, component and elementary functions, which is a design based on user-need (Ahmed *et al.*, 2022).

## Materials and Methods

### Design of the 2-row disc ridger

The fully mounted double-row disc ridger was designed using SOLIDWORKS® Pro. 2019 software and constructed at the Department of Agricultural and Biosystems Engineering workshop of the Kwame Nkrumah University of Science and Technology. The fabricated ridger was tested at the Anwomaso Agricultural Research Station located at latitude 6°41'56.75" N, longitude 1°31'25.85" W and altitude 274 m above sea level.

The double-row disc ridger consists of a 3-point linkage that enables mounting and dismounting of the implement to the tractor for easy transport and operation, a mainframe on which all the parts are mounted, four discs (soil engaging members) arranged in opposite directions, four shanks that connect the discs to the frame, hubs and bearings that enable smooth rotation of the soil engaging members. Hub-wear protectors were incorporated in the ridger bottom sub-assembly to reduce hub base wear. Parts of the hub and disc sub-assembly were procured from implement dealers in the open market to meet heavy-duty primary tillage implement standard.

The design was accomplished using functional analysis and computer aided design method adapted from Abunde (2017) and Yogesh (2007). Value analysis, otherwise known as functional analysis, provides a means of recognizing the need and help define the functions that must be performed. Implicit in this process is the development of an operational concept for the product which is represented by the lower-order functions in a Functional Analysis System Technique (FAST) diagram. Figure 1 presents the methodological framework for the realisation of the ridger. The procedure involved an analysis of need, geometric modelling, fabrication and field testing. Need analysis was done to clarify the fundamental requirement that justifies the design of the disc ridger. The need was validated by considering the questions: Why is there the need for a 2-row disc ridger? What could change the need? What could eliminate the need? A three-dimensional modelling software (SOLIDWORKS® Pro. 19) provided access to the design modelling, simulation and optimization. Figure 2 presents a horned beast diagram that analyzed and defined the needs the implement must meet to help express the design specifications (Zehtaban and Roller, 2012). A FAST diagram which shows how the technical solutions were realized from the need analysis is presented by Figure 3. FAST diagrams are used to prioritize the objectives or functions of a product. Once the objectives were prioritised, it was possible to evaluate the options that lend the most value based on predetermined criteria (Abunde, 2017). The three primary directions indicated on the FAST diagram are: (i) HOW will 'function' be accomplished? (ii) WHY is it necessary to (function)? (iii) WHEN 'function' occurs, what happens?

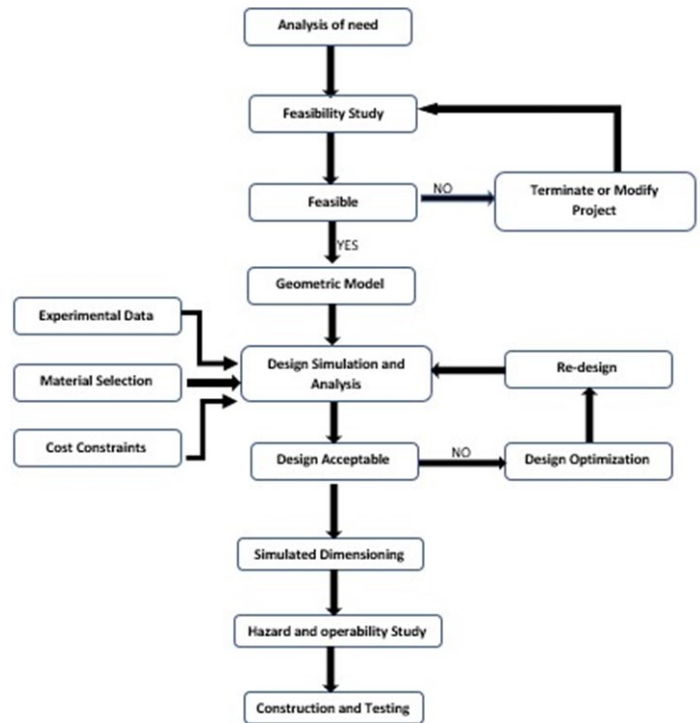


**Figure 1** Workflow of the design and construction process (adopted from Abunde and Jiokap, 2017)

### Functional analyses of need using horned beast diagram

Figure 2 presents a horned beast diagram that clarified the fundamental requirement that justified the design of the double row disc ridger. The diagram is a design project management tool that uses the head of an animal with horns and a protruded tongue to illustrate the need to which the system answered. The head of the animal represented the designed product, the two horns answered the design questions 'who is the beneficiary of the product?', and 'what interactors are concerned?' and the tongue defined the product's goal (Michalakoudis *et al.*, 2017). As indicated in the diagram, the goal of the ridger was to form ridges on arable soil for mechanization of root and tuber cultivation.

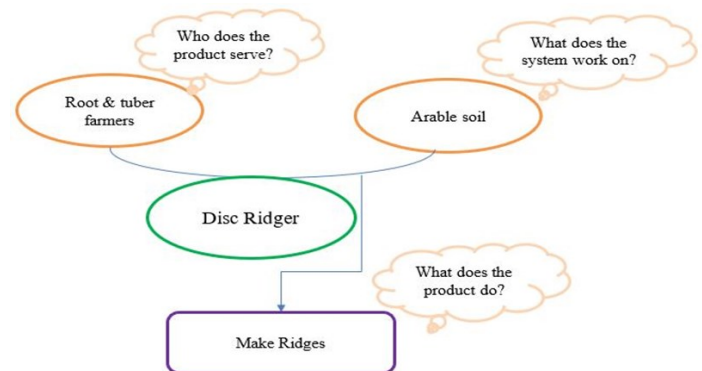


**Figure 2** Horned beast diagram showing functional analysis of the need

**Identification of functions (Octopus diagram)**

Figure 3 presents an Octopus diagram, which comprises the designed product and the different components of its external medium. Unlike the horned beast diagram, which defined the need, the octopus diagram defined the functions that satisfy the need. The functions were broken into principal and constraint functions as shown in Table 1. The designed product is in the centre of the diagram, and the environment's external elements (EE) are positioned around. While the interaction or principal function links to external elements through the product, a constraint or adaptation function links an external element directly to the product (Ahmed *et al.*, 2022). The functions involved in the octopus diagram in Figure 3 are enumerated in Table 1.

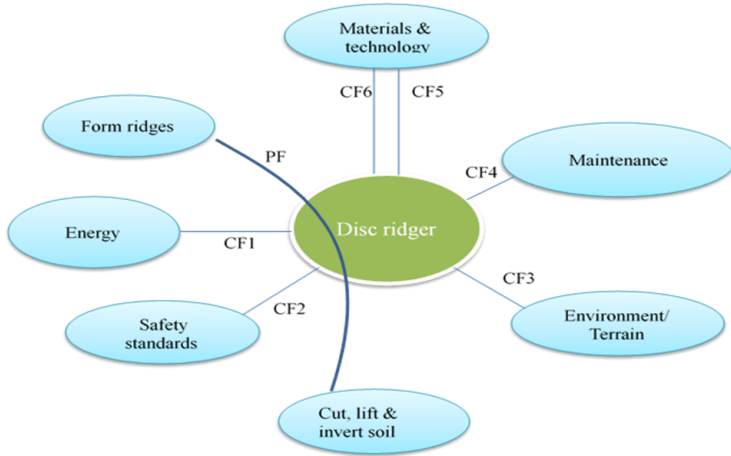


**Figure 3** Octopus diagram showing the relationship between system and external medium

**Table 1** The principal and constraint functions together with their descriptions

Function (F)	Principal (PF)	Constraint (CF)
Make bonds/ridges	PF	
Use draught power from tractor		CF1
Design should respect safety standards		CF2
Design should respect quality standards and minimize losses from accidents		CF3
Strong enough to work in difficult soil conditions		CF4
Maintenance should be simple and easy to carryout		CF5
Easily constructed with local material and technology		CF6
Materials for construction should be of good quality, locally available and cost-effective		CF7

**Functional analyses system technique (FAST diagram)**

A FAST diagram in Figure 4 presents the technological solutions that permit the satisfaction of the principal and constraint functions. The diagram is a graphical representation of the logical relationships between the functions of the ridger. It illustrates how functions were expanded in “How” and “Why” directions as shown by the blue arrowheads. The design specification and technical specification of the ridger are shown in Tables 2 and 3 respectively.

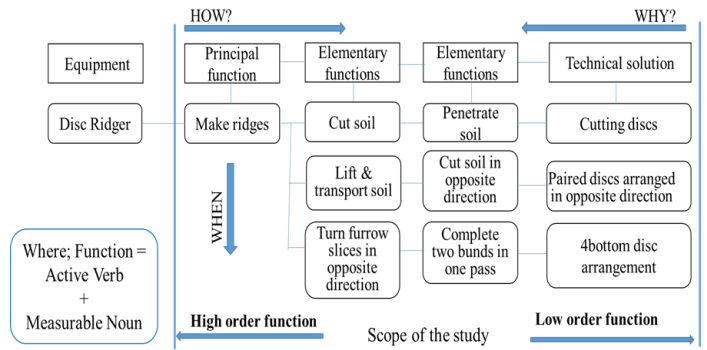


**Figure 4** FAST diagram showing functions and their corresponding technical solutions

**Geometric modelling of the ridger**

Figure 5 presents the orthographic views of the ridger obtained with the SOLIDWORKS® drawing software. These include the plan, front and end elevations. Three-dimensional (3D) views of the main frame and shanks are shown in Figures 6 and 7 respectively.

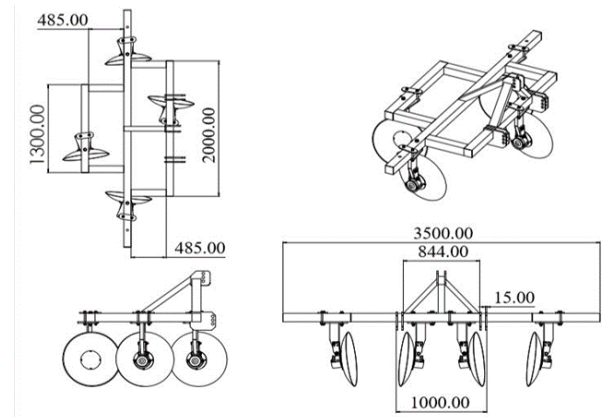


**Figure 5** Orthographic view of disc ridger

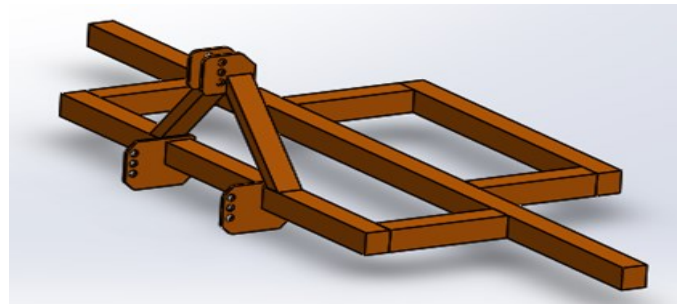


**Figure 6** 3D view of the support frame

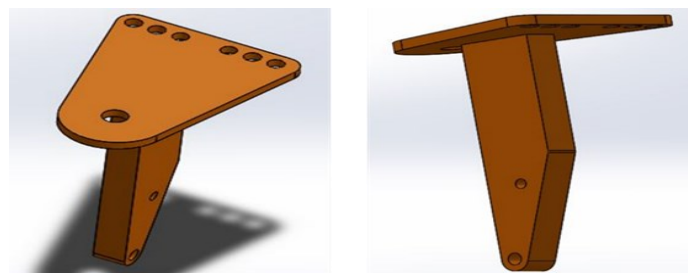


**Figure 7** 3D Views of shank

**Table 2** Design specification manual of the ridger

Item No.	Service Function	Characteristics		Constraints
		Parameter	Specification	
1	Pull ridger through the soil	Power required (HP)	75-110	Use drawbar power from a tractor
2	Hold ridger assembly and allow mounting/dismounting	Frame and 3point linkage construction	Heavy-duty box Frame 100×100×6mm	Operate in tough conditions without structural defects.
3	Penetrate, Cut, lift, transport and invert soil to form bunds	Type and Size of cutting discs	Plain Concave Disc 660×6mm	Rollover obstacles, ensure smooth operation and impose less draught.
4	Allow turning of disc during operation	Weight	435kg (Approx.)	Penetrate soil by its own weight
5	Vary working width and depth	Type of Hubs and bearings	High quality (SAE 52100)	Ensure smooth operation and minimal load on a tractor
		Disc angle	40, 43, 45deg.	Should be easily adjustable
		Spacing between disc	0.5, 0.7, 1m	
		Tilt angle	15, 20 and 25deg.	

**Table 3** Technical specification of the ridger

Item No.	Parameter	Specification
1	Type of ridger	Double row disc ridger
2	Frame construction	Square tubular rigid frame
3	3-point linkage construction	610 x 825mm Triangular frame
4	3-point linkage materials	100 x 50mm mild steel tubular bar
5	Frame materials	100 x 100 x 6mm mild steel frame;
6	Number of bottom/discs	4
7	Size of disc	660 x 4mm
8	Type of disc	Plain circular concave revolving disc
9	Number of bearing hubs	4
10	Type of bearing	Ball-bearing
11	Bearing size outer	60 x 130mm (6312)
12	Bearing size inner	45 x 85mm (62092)
13	Disc angle	Adjustable
14	Tilt angle	Adjustable
15	Size of shanks	40 x 20mm solid rectangular bar
16	Number of shanks	4
17	Maximum width of cut	3500mm
18	Working depth	330mm

**Three-point linkage hitch system**

A category 2 hitch system (82 mm wide and 610 mm high) was designed considering the power available on most farms to pull the implement. The length of the triangle was determined to be 37.7 mm at an angle of 56°.

**Ridger bottom sub-assembly**

The bottom sub-assembly consists of the shank, disc, hub (flange, bearing, bearing cup, seal, and grease) and hub-wear protectors. One of the principles that governed the design process was simplicity. The design had minimum deviations as possible from farmers' traditional tillage implements and components were made compatible with parts of traditional implements. In other words, modifications were made only where necessary. Figures 8 and 9 present an exploded and assembled views of the ridger bottom. Part list of the ridger bottom sub-assembly in Figure 8 is given in Table 4.

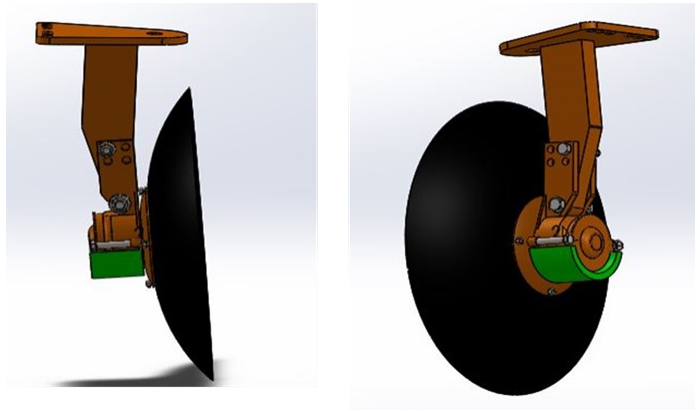


**Figure 9** 3D views of ridger bottom sub-assembly

**Complete ridger assembly**

Figure 10 presents a complete view of the ridger. Part list of the various components of the assembly are shown in Table 5.

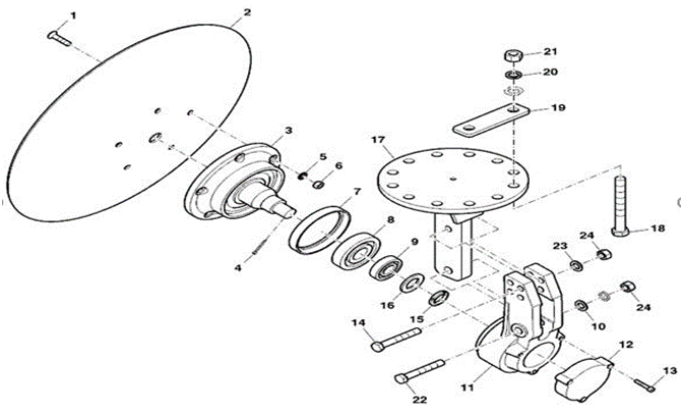


**Figure 8** Exploded view of ridger bottom

**Table 4** Parts identification list of ridger bottom in Figure 8

Item No.	Part	Item No.	Part
1	Bolt	13	Bolt for hub cover
2	Concave disc	14	Hub-shank connecting bolt
3	Flange	15	Castellated nut
4	Lock pin	16	Washer
5	Washer	17	Disc angle adjustment plate
6	Nut	18	Bolt
7	Bearing case	19	Brace
8	Big end bearing	20	Washer
9	Small end bearing	21	Nut
10	Washer	22	Bolt
11	Hub case	23	washer
12	Hub cover	24	Nut

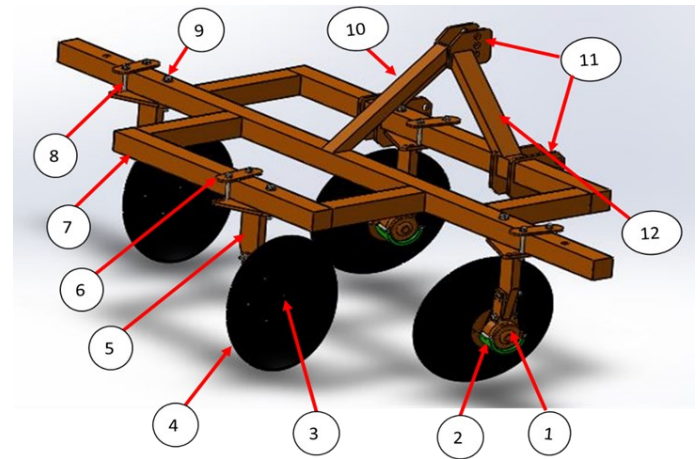


**Figure 10** 3D Labeled assembled view of 2-row disc ridger

**Draught force prediction model for disc implements**

Knowledge of the passive force's horizontal, vertical and lateral components that a tillage implement is likely to encounter under field conditions was necessary during the design process to determine the strength of the material for construction. The draught force prediction model developed by Godwin *et al.* (1987) and cited by Godwin *et al.* (2007) available in literature was used to predict the passive force acting on disc implements. The value of the predicted force was applied as the force required during the simulation stage of the design. The results of SOLIDWORKS® simulation based on the predicted load then informed the basis for materials (quality and size) selected for the construction of the ridger. The passive soil reaction force (P) on a disc was calculated as follows, adapting work by Alam (1989). The disc was assumed to translate horizontally at a disc angle as well as an inclination angle.

$$\text{Passive force (P)} = [Y_i Z^2 K_y + CZK_c + (R - Z)Y_f Z K_q \sin\phi] \times 2(RZ - Z^2)^{0.5} \sin\phi \quad (1)$$

$$\text{Projected width of cut (W)} = \frac{2 \cos\beta}{\cos\alpha} \sqrt{Z(D \cos\alpha - Z)} \quad (2)$$

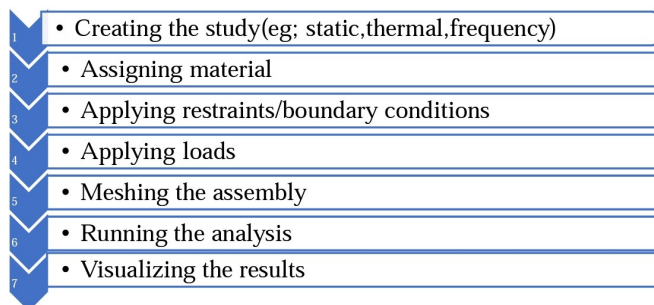
Where R = Disc sphere radius, Z = Depth of cut, β = Disc angle, α = Disc inclination or tilt angle, and K = Dimensionless factors, are all disc properties whereas Y = Bulk unit weight, c = Cohesion, q = Surcharge, φ = Angle of internal friction, and δ = Angle of soil-metal friction are soil properties.

**Table 5** Partlist of in Figure 10 Ridger

Item No.	Part Name	Material	Quantity
1	Hub and bearing	Chrome steel	4
2	Hub wear protector	Mild steel	4
3	Disc bolt	Carbon steel	16
4	Concave disc	Boron steel	4
5	Shank	Mild steel	4
6	Bracket	Mild steel	4
7	Mainframe	Mild steel	1
8	Shank bolt	Carbon steel	8
9	Central bolt	Carbon steel	4
10	3-point linkage stay	Mild steel	1
11	3-point link plate	Mild steel	6
12	3-point link frame	Mild steel	2

### Design simulation

The design simulation was carried out using the procedure outlined in the SOLIDWORKS® Simulation Guide (2010). The procedure for using the guide is outlined in Figure 11.

**Figure 11** Flowchart of the design simulation processes

### Construction of the implement

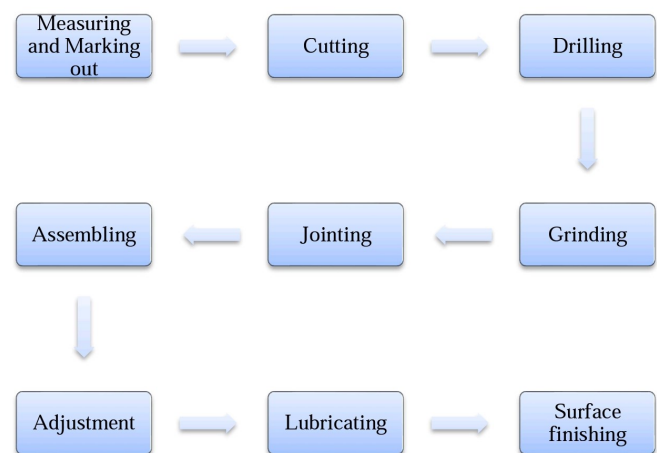
The implement was constructed at the Agricultural and Biosystems Engineering Workshop of KNUST in Ghana. Figure 12 presents the manufacturing processes that led to the construction of the ridger. The disc ridger was built in five stages.

First was the construction of the main frame to carry the soil working members, second was the hitching system to allow the implement to be hitched to the tractor for easy transport and operation, third was the shanks/standard which connects the ridger bottom to the frame and fourth was the hub and discs assembly. The hub and discs assembly are sub-assembly which consists of the discs, flanges, hubs, bearings (these parts were outsourced from implement dealers in the open market) and hub-wear protectors. The final part of the construction was assembling/bolting the components together to form the two-row disc ridger. The main frame was constructed using 100 x 100 x 6 mm tubular pipe made of mild steel. It was first marked into five parts of lengths presented in Table 6.

A full length of square pipe was cut into the seven pieces listed above. Three holes of 30 mm diameter (each) were drilled along both ends of the main bar 1090 mm from the

centre of the 3500 mm bar. These holes were spaced 210 mm apart to allow for working width adjustment. Two holes of the same diameter were drilled 310 mm from the centre of the main bar, one each on the front and back bars of the frame to enable connection of the shanks to the frame. The parts were assembled and welded together to form the mainframe of the ridger. The frame was re-enforced using a 6 mm mild steel plate split 100 x 180 mm (12 pieces) and bend at 90 degrees angles. The angular plates were attached to all 12 corners of the mainframe through a permanent jointing technique (welding). The square holes left at the ends of the frame assembly were covered by welding 100 x 100 x 4 mm mild steel plates welded to each hole. The welded parts of the frame were neatly dressed using a power grinding machine.

One full length of 100 x 50 x 6 mm mild steel hollow pipe and pieces of 16 mm mild steel plate were used to construct the 3-point linkage hitch system. Two pieces of the 50 x 100 mm pipe were cut to the length calculated above and welded to form a triangle with the front side of the mainframe.

**Figure 12** Manufacturing process flowchart

**Table 6** Dimensions of parts used to construct the mainframe

Item No.	Part	Unit	Dimension (mm)
1	Main bar	1	3500
2	Lead/front bar	1	2000
3	End/back bar	1	1300
4	Connecting/link bar	4	600

Six pieces of 16 mm plate were cut to form 100 x 175 mm right angle and chamfered at the ends. These plates were welded in two pairs, spaced at 100 mm attached to the ends of the triangle to form the three-point linkage system, providing one top and two lower link hitch points. The front bar of the mainframe completed the triangle of the linkage. A stay of wedge 270 x 200 mm was cut out of 50 x 100 mm pipe and welded to connect the top-link hitch point to the main bar to ensure stability of the hitch system. Three holes of diameter 30 mm were drilled on each plate to accommodate hitch pins. The mainframe of the ridger was then completed as shown in Figure 6.

The shanks (four pieces) were constructed with a 100 x 40 mm mild steel bar, chamfered at the bottom end with a chamfer distance of 170 mm as shown in Figure 3.8. Triangular plates (Four pieces) of 300 x 240 mm were cut out of 16 mm mild steel plate and placed on top of each shank with holes drilled through them to enable connection to the mainframe and adjustment of the disc angles. Figure 3.8 presents the 3D view of the shank.

For purposes of replacement, the disc, hub and bearing design were made compatible with existing implements. The diameter of the hub was measured, and semi-circular wear protectors cut (200 mm length, 90 mm wide and 16 mm thickness), rolled and welded to the base of the hubs to prevent wear, due to inevitably deep working depths during operation on undulated fields. The various components of the sub-assembly were joint together by bolts and nuts.

## Performance testing of the ridger

### Experimental area

The fabricated implement was tested for field performance on an area of 5775 m<sup>2</sup> (165 x 35 m) equivalent to 0.58 hectares of land. The site was first cleared of top growth, ploughed and harrowed before ridging experiment began.

### Materials/Equipment

Prior to the performance test, soil samples from the location were taken from depth (0 - 30) cm by an auger. The soil at the experimental site was generally clay-loam. Other materials used include:

- Measuring tape: An iron 50-meter measuring tape was used for measuring dimensions and distances, to calculate areas and speeds.
- Steel poles: Used for marking the distances during the experiment.
- Stopwatch: Used to determine the tractor speed and recording time.
- Measuring cylinder: One-litter capacity graduated cylinder was used to refill the fuel tank for determination of fuel consumption.
- Fuel jerry can: It was used for transporting fuel to the field.
- Steel pipe with hooks at both sides: Used for pulling the tested tractor by the auxiliary one.

vii. Dynamometer: Dynamometer with 3000kg was used for direct draft measurement.

viii. Notepad: Recording the data and drawing the map of work.

ix. Tractors: two tractors were employed to carry out the evaluation of the implement. The tractors used for the experiment were VALTRA (shown in Plate 1) and New Holland, both with 55.95 kW rating. The specifications of the tractors are shown in Table 7.

**Table 7** Specification of Tractors

Specification	Tractor (1)	Tractor (2)
Model	Valtra 795	New Holland 290
Make	4WD	4WD
Engine type	Diesel	Diesel
No. of cylinders	4	4
Cooling system	Water-cooled	Water-cooled
Engine power	75 hp	75 hp

**Plate 1** Experimental tractor

### Field measurements

The following field measurements were taken during performance testing:

#### (a) Measurement of draught force

Implement draught was determined for each run of ridging using a 10-tonne RON 2125 Dynamometer (Plate 2). The instrument is equipped with a data-logger, which stores the force (kN) required to pull each implement, making it possible to download stored data onto the computer for analysis using popular spreadsheet programs. The instrument was linked to a towing bar placed between two tractors. The instrumented tractor had the implement hitched to it and set to a neutral gear and pulled by another tractor. Load and no-load draught forces were obtained for runs in working and transport positions respectively.



**Plate 2** RON 2125 Dynamometer

Plate 3 shows the implement draught measurement procedure with one tractor pulling the other with the ridger hitched to it and the force required for pulling being logged onto the RON 2125 Dynamometer. Step-by-step procedure for measuring implement-draught are as follows (Serrano, *et al.*, 2007): (1) The dynamometer was attached to the front of the tractor to which the implement was hitched; (2) An auxiliary tractor was linked to the test-tractor through the dynamometer with a chain, which allowed the auxiliary tractor to toe the test-tractor, stretching the dynamometer. The draught force (kN) was recorded for a measured distance of 165 m at no load; (3) The implement was put in tillage position (loaded) and the rear tractor was pulled to record the draught force. The difference between the two readings gives the value of the draught required to pull the implement. The draught force (kN) was calculated using equation (3):

$$P = P_2 - P_1 \quad (3)$$

Where  $P$  = draught force,  $P_1$  = force required to pull the implement in transportation position, and  $P_2$  = force required to pull the implement during tillage operation.

Specific draught ( $N/m^2$ ) to pull the implement is mathematically expressed by equation (3):

$$\text{Specific draught (n)} = \frac{P}{A} \quad (4)$$

Where  $P$  is actual draught in N and  $A$  is area ploughed in  $m^2$ .

In other words, the average drawbar-pull (draught to pull the implement) is the difference between the towing forces while in neutral gear without the implement in tillage operation and the towing force while the implement is in tillage operation, respectively.

*(b) Measurement of depth and width of cut*

The depth and width parameters were determined by setting the hydraulic control lever that controls the lifting mechanism at a level corresponding to the required depth of cut and driven at predetermined speeds (1.67 – 2.23 m/s). The depth of cut (height of ridge) was measured with a steel tape, from the

bottom of the furrow to the surface level of the soil at randomly selected points.

*(c) Rear-wheel slippage*

The rear-wheel slippage was determined using un-ridged area to represent normal working conditions. The rear wheel was marked with chalk at a position tangential to the ground surface. A distance covered by ten (10) revolutions of the rear-wheel was recorded with the tractor under no-load condition. Another distance covered by the same number of wheel revolutions was measured with the tractor fully engaging the ridger in the soil. The wheel slippage was calculated as follows:

$$\text{Wheel-slippage (\%)} = \frac{\text{Revolutions with load (m)} - \text{Revolutions without load (m)}}{\text{Revolutions with load (m)}} \times 100 \quad (5)$$



**Plate 3** Tractors–dynamometer, implement mounted in tillage operation

*d) Measurement of field capacities and efficiencies*

A distance of 165 m was measured on the plot. Rigging started at the required speed; the width of cut was measured with a tape. Time (sec) for each operation was recorded with a stopwatch. Time for turning was also measured for the plot. Theoretical Field Capacity (TFC), Effective Field Capacity (EFC) and Field Efficiency (FE) were calculated using equation 7, 8 and 9:

$$\text{TFC (ha/hr)} = \frac{S \times W}{C} \quad (6)$$

$$\text{EFC (ha/hr)} = \text{TFC} \times \text{FE} \quad \text{or} \quad \text{EFC} = \frac{A}{t} \quad (7)$$

$$\text{FE} = \frac{\text{EFC}}{\text{TFC}} \times 100 \quad (8)$$

Where FE is the field efficiency (%),  $S$  is the average speed (km/hr),  $W$  is the average width of cut,  $C$  is the constant (8.83) (Abdalla *et al.*, 2014),  $t$  is the average working time (hr) (time includes non-productive time), and  $A$ , the area covered (ha)

*(e) Measurement of fuel consumption*

The tractor started working the plot with a full tank capacity. After finishing the operation, the tank was refilled by a measuring cylinder and the quantity of fuel used to refill the tank was recorded. The fuel consumption was calculated in litre/ha as follows:

$$\text{Consumption (l/ha)} = \frac{\text{Reading of Cylinder (ml)}}{\text{Area of Plot (Ha)} \times 1000} \quad (9)$$



### (f) Determination of soil moisture content

Prior to the field test, soil samples were collected at depth of 0–30 cm, 30–50 cm and 50–70 cm with the aid of soil auger at three replications per sample points for determination of soil parameters. Field test samples were randomly selected for the determination of soil moisture content using the oven-dry method (gravimetric). The moisture content of the soil was obtained using equation 10.

$$\text{Moisture Content (\%)} = \frac{W_w - W_D}{W_D} \times 100 \quad (10)$$

Where  $W_w$  = weight of wet soil sample, g,  $W_D$  = weight of dry soil sample, g

### (g) Measurement of soil penetration resistance (cone index)

The soil cone index (CI) was measured to ascertain the soil strength profile using AGRETO Soil Compaction Tester having an enclosed angle of  $30^\circ$ , with a base area of  $3.23 \text{ m}^2$  ( $323 \text{ mm}^2$ ), mounted on a shaft of 0.203 cm (20.27 mm) marked with respect to depths on the shaft. At three different depths (0–100, 100–150, and 150–200) mm, soil resistance (cone index) to the penetration of implements were obtained before tillage operation. Cone penetrometer testing involved pushing a cone into the soil at a steady rate and recording the resisting force exerted by the soil on the penetrometer. The force recorded by the dial is divided by the base area of the cone to provide a “pressure” measurement, referred to as cone index in  $\text{KN/m}^2$ .

### Data collection and analysis

SOLIDWORKS® Pro 19 was used to run design simulation analysis and the data collected from the experiment was subjected to an ANOVA test using MATLAB 2019 at a significance level of  $\alpha = 5\%$ .

## Results and Discussion

### The designed and fabricated 2-row disc ridger

The object of this project was to develop and test a fully mounted double-row disc ridger for root and tuber crop production. The design and constructional procedure laid down in the material and methods was followed to realise the implement. Plate 4 presents the finished view of the developed ridger.



**Plate 4** The fabricated fully mounted double row disc ridger ready for testing

### Design simulation

Figure 13 presents Von Mises stresses obtained from the finite element analysis. The minimum and maximum stresses obtained were  $1.867\text{e-}02 \text{ N/m}^2$  and  $5.141\text{e+}06 \text{ N/m}^2$

respectively and the yield strength of the material was  $6.204\text{e+}08 \text{ N/m}^2$ . This result proved that the prototype design was valid and safe and could withstand the stresses from predicted field conditions. This conclusion was drawn because the design met the requirement of Von Mises yield criterion, which states that if the Von Mises stress of a material under load is equal or greater than the yield limit of the same material under simple tension, the material will yield or fail (Capecchi and Ruta, 2015; Capecchi and Ruta, 2016).

The result obtained in the experimental tests also validated the design of the ridger since the measured draught force of 1.8 – 2.4 kN was lower than the 3.75 kN predicted force that was applied during the design simulation. The method of simulating the performance of the implement by introducing static loads on the mainframe was appropriate because the numerical results were well correlated to those obtained from the experimental tests.

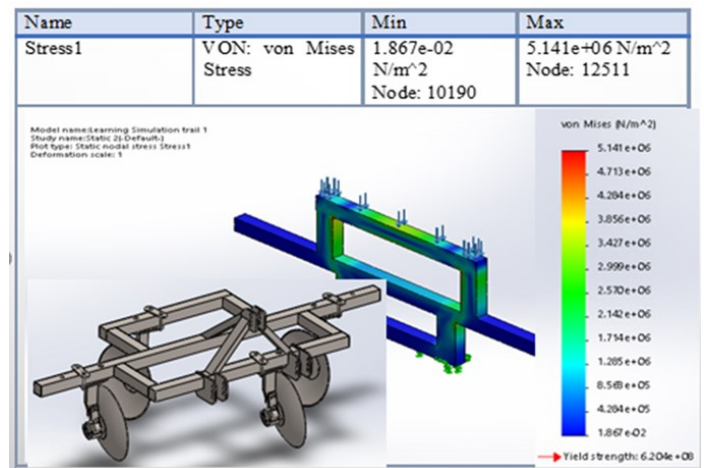


**Figure 13** SOLIDWORKS® simulation study results

### Field test of the ridger

#### Soil moisture content

Figure 14 shows the moisture content of the selected site prior to the field test. It was observed that the moisture content increased steadily with depth from 0 to 12 cm and decreased sharply from 12 to 30 cm deep. The highest moisture content of the soil was recorded at 10 cm depth. The average moisture content of 13 % was recorded prior to the field test. This moisture content was within acceptable limits for tillage as reported by Kumi (2011) who mentioned that it is advisable to till the land at a low moisture content at the beginning of rains when the moisture content is usually between 5 % and 15 %.

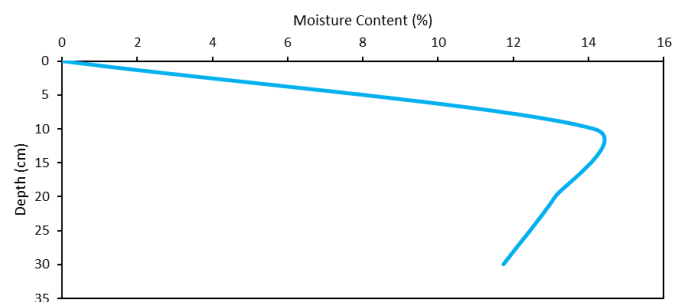


**Figure 14** Moisture content of the field prior to evaluation

### Soil penetration resistance before and after ridging

Figure 15 presents the soil penetration resistance before and after ridging. The results indicate a trend of increasing resistance with probing depth. In other words, as the depth of probe increased, so did resistance to penetration as shown on the graph. This observation means, the deeper the ridger engages the soil, the more resistance it will encounter, which influence draught force imposed on the tractor-implement, wheel-slip, and fuel consumption. The highest resistance of 155 kN was observed at a depth of 25 cm before ridging operation and reduced sharply from 155 to 140 kN at probing depths of 26 to 30 cm. A similar trend was observed after the ridging. However, a reduction in soil penetration resistance was recorded after the ridging operation, the highest resistance being 145.6 kN at 25 cm depth of probe. What is worth noting here is that the ridging operation caused further disintegration or loosening of the soil, which accounted for the 10 kN reduction in penetration resistance recorded by the cone penetrometer.

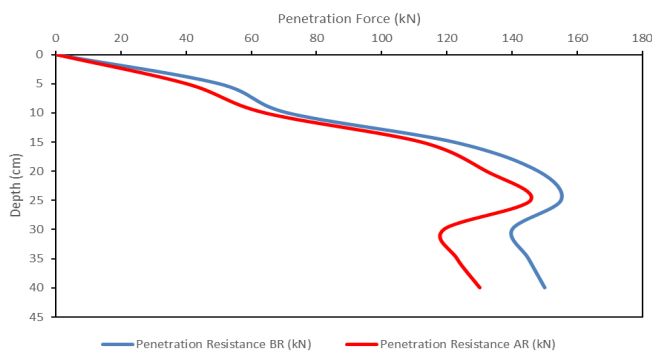


**Figure 15** Soil penetration resistance before and after ridging

### Measured performance during field testing

Figure 16 presents the profiles of load and no-load draught forces recorded during field testing of the ridger. The no-load draught force was recorded with the implement in transport position and the load-draught force was taken when the ridger engaged the soil (during ridging). An average net draught force of 2.2 kN was recorded.

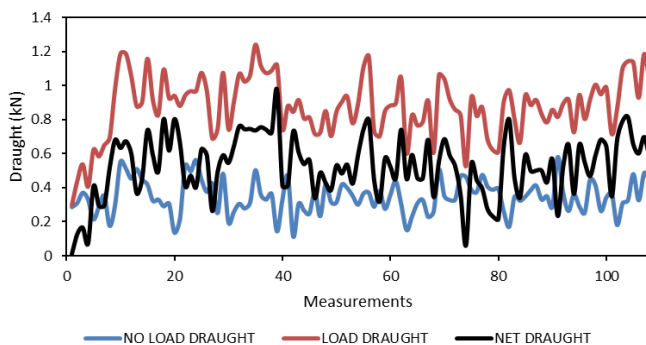


**Figure 16** Profile of load and no-load draught forces recorded during field testing

### Effect of tractor speed on ridger performance

Figure 17 presents the effect of tractor speed on draught force (kN), fuel consumption (l/ha), wheel-slip (%), depth and width of cut (cm). A minimum and maximum draught force of 1.8 and 2.4 kN, respectively were recorded at varied ridging speed from 6 – 9 km/h. These values indicate optimum performance as they fall within the predicted and measured draught force for disc implements computed by the ASABE (2000). The results

revealed a slight increase in draught force (1.8 – 2.4 kN) as speed increased. It is intriguing to note that the minimum draught force was recorded at 8 km/h tractor speed. This means that high draught force is required when ridging at speeds below 8 km/h and above 9 km/h. Regardless of the slight increase in the draught, field tests recorded an  $R^2$  of 0.199, indicating less significance of the effect of speed on draught force, which totally agrees with findings of Tayel *et al.* (2015). This may be attributed to the rotation of the discs, which absorbs part of the soil forces at a certain speed.

Average fuel consumption recorded was 6.35 l/ha. The highest fuel consumption of 7.04 l/ha was recorded at tractor speed of 9 km/h and lowest of 5.41 l/ha at 8 km/h tractor speed. It is apparent from the graph that increased speed resulted in increased fuel consumption. These measured fuel consumption values agree with the American Society of Agricultural Engineers (ASABE, 2000) standard of 9 l/h of average fuel consumption for disc implements. While these results agree with literature, suggesting that increased speed results in increased fuel consumption (Nkakini, 2015; Mamkagh, 2019), the effect was not significant, giving an  $R^2$  of 0.1992.

The minimum and maximum wheel-slip of 5.5 and 5.7% were recorded at tractor speed of 6 – 9 km/h respectively. This is not as significant as the 15 % stated in some literature. However, the results agree with the 5.7 % wheel-slip recorded by Abdalla *et al.* (2014).

Depth and width of cut rather saw a significant increase with an increase in tractor speed given an  $R^2$  of 0.85 and 0.70 respectively. The observed increase in depth of cut as a function of speed indicates that at high forward speed, better and conical ridges are formed. In other words, heaping is best at high speed than at low speed. While it is yet unclear what might have accounted for the increase in width of cut at increased speed; the possible explanation is that there is a clear demarcation of furrows at high speed.

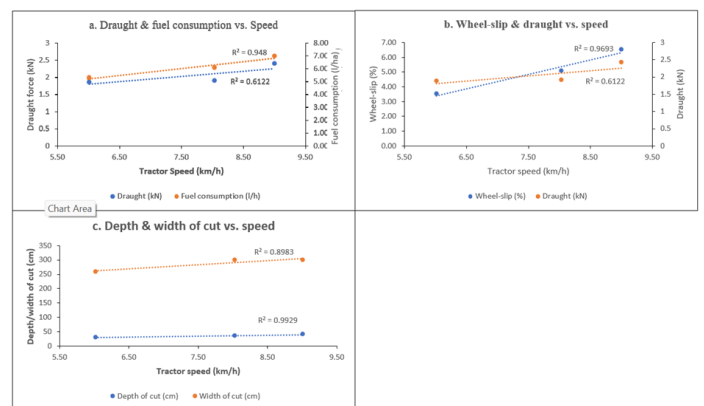


**Figure 17** Effect of tractor speed on ridger performance

### Effect of disc angle on ridger performance

Contrary to the observations made in Figure 17, Figure 18 presents a rather significant effect of disc angle on draught force (kN), fuel consumption (l/ha), wheel-slip (%), depth and width of cut (cm). The results revealed an  $R^2$  of 0.98 for draught, 0.90 for fuel consumption and 0.912 for wheel-slip indicating a significant effect of disc angle on these performance parameters. This agrees with research by Joshton and Birtwistle (1963), Mamkagh (2009), Nkakini (2014) and Abdalla *et al.* (2014), stating that an increase in disc angle results in an increase in draught force, wheel-slip and fuel consumption.

Also,  $R^2$  of 0.81 and 0.85 were recorded for depth and width of cut respectively. This apparently shows that depth and

width of cut increased significantly as disc angle increased. As explained earlier, an increase in depth of cut indicates as disc angle increased, better and conical ridges are formed, and that clear demarcation of furrows are observed. These findings are also in line with the body of literature suggesting that an increase in disc angle results in increase in depth and width of cut respectively (Abdalla *et al.*, 2017; Askari and Khalifahamzehghasem, 2013; Moenifar *et al.*, 2014). This was mainly because a huge volume of soil was conveyed by the disc when the disc angle increased and vice-versa.

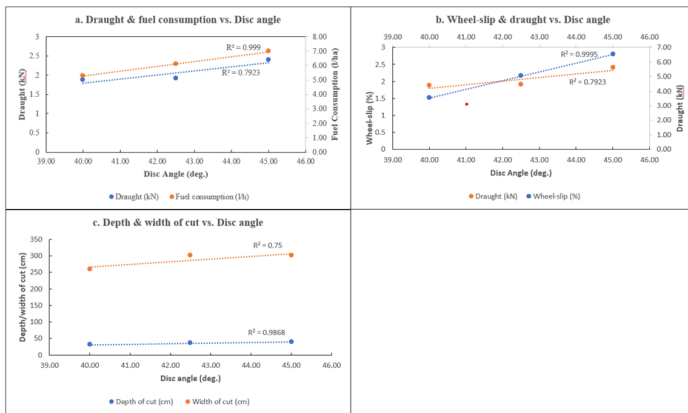


**Figure 18** Effect of disc angle on ridger performance

## Conclusions

A fully mounted double-row disc ridger has been developed and tested. The study applied functional analysis and computer aided design methodology in the design of the tillage implement for local application. A key advantage of this methodology is that it aligns the specification of the device to the requirements of the users thereby streamlining wasteful functionalities and, hence, reducing the cost of manufacturing. The device was fabricated from locally available materials and tools, making it an adaptable, resilient and affordable technology for local artisans and small-scale farmers who contribute 90 % of root and tuber crops in Ghana.

Preliminary field tests were conducted to determine the response of the implement to performance parameters such as draught, wheel slip, fuel consumption, depth and width of cut. Additional conclusions that can be drawn are that the design meets the requirement of its service function with a field capacity of 1.45 ha/h and fuel consumption of 6.3 l/ha; optimum performance of the disc ridger was achieved at a disc angle of 42.5° and tractor speed of 8 km/h with tilt angle set at 25°; and increase in disc angle (40° - 45°) and tractor speed from 6 - 9 km/h resulted in increased draught force from 1.8 - 2.4 kN. However, tractor speed had no significant effect on draught as an  $R^2$  of 0.199 was recorded, indicating less variation; fuel consumption increased from 5.23 - 7.04 l/ha with an increase in disc angle and tractor speed; and depth and width of cut increased from 30 - 40 cm and 240 - 280 cm, respectively, with a corresponding increase in tractor speed and disc angle.

This study recommends further evaluation to establish the effect of different moisture contents and soil type on the performance of the ridger. Wear and durability tests of the ridger on different agro-ecologies are also recommended. Finally, since the current design is meant to ease constraints associated with mechanical harvesting, an interesting progression of the study should focus on assessing the extent to which ridges made by the disc ridger can accommodate mechanical harvesting.

## Acknowledgements

The authors wish to thank the Kwame Nkrumah University of Science and Technology for providing equipment and technical support, and Mr. Abebrese Kwabena Agyeman of Ministry of Food and Agriculture (MoFA), Tamale, Ghana for his time and material support during the research.

## Conflict of Interest Declaration

The researchers declare no conflict of interest.

## References

- Abdalla, O. A., Hamid, A. I., El Naim, A. M. and Zaied, M. B. (2017). Tractor Performance as Affected by Tilt Angle of Disc Plough under Clay Soil. In Science and Technology Publishing (SCI and TECH) (Vol. 1). <https://www.researchgate.net/profile/Ahmed-El-Naim/publication/315667463>
- Abdalla, O. A., Mohamed, E. A., El Naim, A. M., El Shiekh, M. A., and Zaied, M. B. (2014). Effect of disc and tilt angles of disc plough on tractor performance under clay soil. *Current Research in Agricultural Sciences*, 1(3), pp. 83-94.
- Abdullah, A.A. and Rahman, M.S.A. (2019). Comparison between local manufactured panel ridge and conventional disc ridge throughout investigating their effects on power-use-efficiency, draft force and actual field productivity. *Tikrit Journal for Agricultural Sciences Magallaʿ Tikrīt li-l-ʿulūm al-zirāʿat*, 19(1), pp.126-141. DOI: <http://dx.doi.org/10.25130/tjas.v19i1.360>
- Abunde Neba, F., and Jiokap Nono, Y. (2017). Modelling and simulated design: A novel model and software of a solar-biomass hybrid dryer. *Computers and Chemical Engineering*, 104, pp. 128-140. <https://doi.org/10.1016/j.compchemeng.2017.04.002>
- Ahmed, B. S., Benbouzid, S., and Nibouche, F. (2022). Design and implementation of smart glasses with ISMS and risk management functionalities for a technical operator. *Ingénierie des Systèmes d'Information*, 27(3). <https://doi.org/10.18280/isi.270307>
- Alam, M. M. (1989). Soil reaction forces on agricultural disc implements. Doctoral dissertation, Newcastle University, Newcastle.
- Amponsah, Shadrack K., Bobobee, E. Y. H., Agyare, W. A., Okyere, J. B., Aveyire, J., King, S. R., and Sarkodie-Addo, J. (2014). Mechanical cassava harvesting as influenced by seedbed preparation and cassava variety. *Applied Engineering in Agriculture*, 30(3), pp. 391-403. <https://doi.org/10.13031/aea.30.10495>
- Amponsah, S. K., Addo, A., and Gangadharan, B. (2017). Review of various harvesting options for cassava. In *Cassava*. IntechOpen. <https://doi.org/10.5772/intechopen.71350>
- ASABE. (2000). American Society of Agricultural Engineers.
- Askari, M., and Khalifahamzehghasem, S. (2013). Draft force inputs for primary and secondary tillage implements in a clay loam soil. *World Applied Sciences Journal*, 21(12), pp. 1789-1794. <https://doi.org/10.5829/idosi.wasj.2013.21.12.2595>
- Capecchi, D., and Ruta, G. (2015). The theory of elasticity in the 19th century. In *Strength of Materials and Theory of Elasticity in 19th Century Italy* (pp. 1-81). Springer, Cham. [https://doi.org/10.1007/978-3-319-05524-4\\_1](https://doi.org/10.1007/978-3-319-05524-4_1)
- Capecchi, D., and Ruta, G. (2016). Strength of materials and theory of elasticity in 19th century Italy. Springer International Pu. <https://doi.org/10.1007/978-3-319-05524-4>

- Diao, X., Silver, J., and Takeshima, H. (2016). Agricultural mechanization and agricultural transformation (Vol. 1527). Intl Food Policy Res Inst. <https://ebrary.ifpri.org/digital/collection/p15738coll2/id/130311>
- Ennin, S. A., Otoo, E., and Tetteh, F. M. (2009). Ridging, a mechanized alternative to mounding for yam and cassava production. *West African Journal of Applied Ecology*, 15, 3785. <https://doi.org/10.4314/wajae.v15i1.49424>
- Godwin, R. J. (2007). A review of the effect of implement geometry on soil failure and implement forces. *Soil and Tillage Research*, 97(2), pp. 331-340. <https://doi.org/10.1016/j.still.2006.06.010>
- Godwin, R. J., Seig, D. A., and Allott, M. (1987). Soil failure and force prediction for soil engaging discs. *Soil Use and Management*, 3(3), pp. 106-114. [doi.org/10.1111/j.1475-2743.1987.tb00719.x](https://doi.org/10.1111/j.1475-2743.1987.tb00719.x)
- Gohad, S. (2018). Hazard and operability study (Hazop) and Hazard analysis (Hazan). Available: <https://doi.org/10.1088/1757-899X/36/1/012003>
- Johnston, R. C. R., and Birtwistle, R. (1963). Wheatland disc plough investigations. II. Discs forces. *Journal of Agricultural Engineering Research*, 8(4), pp. 312-326.
- Kumi, F. (2011). Development and evaluation of an abrasive wear test equipment. Mphil Thesis, KNUST, Kumasi.
- Mamkagh, A. M. (2019). Effect of soil moisture, tillage speed, depth, ballast weight and, used implement on wheel slippage of the tractor: a review. *Asian Journal of Advances in Agricultural Research*, pp 1-7. <https://doi.org/10.9734/AJAAR/2019/46706>
- Mamkagh, A. M. (2009). Effect of ploughing speed, disk angle and tilt angle on farm tractor wheel slip and on ploughing depth using disk plough. *Jordan J. Agric. Sci*, 5(3), pp. 352-360. <https://journals.ju.edu.jo/JJAS/article/view/880>
- Michalakoudis, I., Childs, P., Aurisicchio, M., and Harding, J. (2017). Using functional analysis diagrams to improve product reliability and cost. *Advances in Mechanical Engineering*, 9(1), 168781401668522. <https://doi.org/doi.org/10.1177/1687814016685223>
- Moenifar, A., Mousavi-Seyedi, S. R., and Kalantari, D. (2014). Influence of tillage depth, penetration angle and forward speed on the soil/thin-blade interaction force. *Agricultural Engineering International: CIGR Journal*, 16(1), pp. 69-74. <https://cigrjournal.org/index.php/Ejournal/article/view/2613>
- Nanbol, K. K., and Namu, O. (2019). The contribution of root and tuber crops to food security: A review. *J. Agric. Sci. Technol. B*, 9, pp. 221-233. <https://doi.org/10.17265/2161-6264/2019.04.001>
- Nkakini, S. O. (2015). Draught force requirements of a disc plough at various tractor forward speed in loamy sand soil, during ploughing. *Int. J. Adv. Res. Eng. Tech*, 6(7), pp. 52-68. [https://d1wqtxtslxzle7.cloudfront.net/47787018/IJARET\\_06\\_07\\_008-libre](https://d1wqtxtslxzle7.cloudfront.net/47787018/IJARET_06_07_008-libre).
- Nkakini, S. O., and Akor, A. J. (2012). Modelling tractive force requirements of wheel tractors for disc ploughing in sandy loam soil. *International Journal of Engineering and Technology*, 2(10), pp. 374-385. <https://www.researchgate.net/profile/Silas-Nkakini-2/publication/342721004>
- Nkakini, S. O. (2014). Performance evaluation of disc ridging tractive force model in loamy sand soil using sensitivity measured parameters. *Agricultural Engineering International: CIGR Journal*, 16(2), pp. 15-21.
- Sanginga, N., and Mbabu, A. (2015, October). Root and tuber crops (cassava, yam, potato and sweet potato). In proceedings of an action plan for African Agricultural Transformation Conference, Dakar, Senegal (pp. 21-23). <https://www.afdb.org/fileadmin/uploads/afdb/Documents/Events/DakAgri2015>
- Serrano, J. M., Peça, J. O., da Silva, J. M., Pinheiro, A., and Carvalho, M. (2007). Tractor energy requirements in disc harrow systems. *Biosystems Engineering*, 98(3), pp.286-296. <https://doi.org/10.1016/j.biosystemseng.2007.08.002>
- Sims, B., and Kienzle, J. (2016). Making mechanization accessible to smallholder farmers in sub-Saharan Africa. *Environments*, 3(2), 11. <https://doi.org/10.3390/environments3020011>
- Tayel, M. Y., Shaaban, S. M., and Mansour, H. A. (2015). Effect of ploughing conditions on the tractor wheel slippage and fuel consumption in sandy soil. *International Journal of ChemTech Research*, 8(12), pp.151-159 <https://www.researchgate.net/profile/Said-Shaaban>
- Wang, J., Wang, J., Kong, Y., Zhang, C., and Zhao, J. (2013). Development and experiment of suspension ridger and its key components for paddy field. *Transactions of the Chinese Society of Agricultural Engineering*, 29(6), pp. 28-34. <https://www.ingentaconnect.com>
- Yogesh, J. (2007). Design and optimization of thermal systems, second edition, Library of Congress Cataloging-in-Publication Data Taylor and Francis Group, New York. <https://doi.org/10.1201/9781420019483>
- Zehtaban, L., and Roller, D. (2012). Systematic functional analysis methods for design retrieval and documentation. *International Journal of Computer and Information Engineering*, 6(12), pp. 1711-1716. [doi.org/10.5281/zenodo.1330343](https://doi.org/10.5281/zenodo.1330343)